Axial Dispersion Plug Flow Model for Methanol Dehydration Reactor

Masoud Habibi Zare (masoud.habibizare@yahoo.com)
Isfahan University of Technology
Mohammad Davar Mahlouji
Amirkabir University of Technology

Research Article

Keywords: Axial dispersion, Fixed bed reactor, Methanol dehydration, Dimethyl ether

Posted Date: January 18th, 2021

DOI: https://doi.org/10.21203/rs.3.rs-144105/v1

Axial dispersion plug flow model for methanol dehydration reactor

Mohammad Davar Mahlouji [1], Masoud Habibi Zare[2*]

[1]Chemical Engineering Department, Amirkabir University of Technology, Tehran, Iran

[2]Isfahan University of Technology, Department of Chemical Engineering, 84156-83111 Isfahan, Iran

[*]Corresponding author; E-mail: masoud.habibizare@yahoo.com

Abstract

One-dimensional heterogeneous dispersed plug flow (DPF) model is employed to model an adiabatic fixed-bed reactor for the catalytic dehydration of methanol to dimethyl ether (DME). The mass and heat transfer equations are numerically solved for the reactor. The concentration of the reactant and products and also the temperature varies along the reactor, therefore the effectiveness factor would also change in the reactor. We used the effectiveness factor that was simulated according to the diffusion and reaction in the catalyst pellet as a pore network model. The predicted distribution for the effectiveness factor was utilized for the reactor simulation. The simulation results were compared to the experimental data and a satisfactory agreement was confirmed.

Keywords: Axial dispersion, Fixed bed reactor, Methanol dehydration, Dimethyl ether

1. Introduction

DME is a linear combination, odorless, colorless component and has no corrosive properties. It is also not environmentally hazardous. DME, as a liquefied gas has characteristics similar to those of liquefied petroleum gas (LPG) [1-2]. It is identified as a potential diesel and cooking fuel. Its oxygen content is 34.78% and can be burned without soot emission. It has a boiling point of −25 °C, which is 20 °C higher than LPG and can be liquidized at 0.54 MPa (20 °C).

DME behaves as a gas in standard conditions (0.1 MPa, 298K) [2].

DME can be produced from a variety of feed-stocks such as natural gas, crude oil, residual oil, coal, waste products and bio-mass [1]. One of the commercially processes for DME production is the catalytic dehydration of methanol. For this reaction, acidic porous catalysts such as zeolites, silica–alumina, alumina and etc. are used [3-10]. The reaction rate for this process has been mostly derived from the experiments conducted in the conditions not found in an industrial Reactor [11-15]. Bercic and Levec reviewed the different reaction rates and they designed some experiments to study this reaction in industrial conditions using γ-alumina as the catalyst [12]. The experiments were carried out in a differential reactor (8-mm inside diameter) in a temperature range of 290-360 °C. The pressure was kept constant at 146 kPa. The reactor was operated free of inter particle heat and mass resistances. Bercic and Levec suggested the kinetics of the reaction at this condition [12].

They also used a laboratory scale reactor to find its conversion and temperature profile in it. Then plug flow condition and longitude changes of concentration and temperature were considered for the reactor modeling. They considered convection and reaction terms in the mass and heat transfer equations. In order to find the effectiveness factor, the continuum model was considered for the spherical catalyst particles. They used a Rang Kutta method to solve the mass and heat transfer equations simultaneously [16].

In the modeling presented in this paper we used the results of pore network model for the value of the effectiveness factor. In fact, since the catalyst pellet has porous structure, continuum models cannot predict its behavior precisely.

Any porous structure can be mapped into a pore network model. The pore network models have been extensively used in the last decades. The structure of the porous medium can strongly affect its characteristics. The effectiveness factor was found based on a three dimensional pore network model for the catalyst pellets [17].

Here, we first explain the mathematical model for and the mass and heat transfer process in the reactor. And the mathematical approach for solving the equations is described as well. After that the results are presented and discussed. In the final part a summary of the paper is presorted.

2. Mathematical Model

The dehydration of methanol is based on the following reversible reaction:

$$2CH_3OH \leftrightarrow C_2H_6O + H_2O \quad (1)$$

The reaction rate $(-r)$ is considered as follows [16]:

$$-r = K_s \frac{K_M^2\left(C_M^2 - \frac{C_D C_M}{K}\right)}{\left(1+2\sqrt{K_M C_M}+K_W C_W\right)^4} \quad (2)$$

The kinetic constants and thermodynamics equilibrium constant are presented in Table 1.

Table 1: The kinetic constants

Kinetics parameters	Value
K_S [16]	$5.35\times10^{13}\exp(-17280/T)\ \ (kmol/kg.hr)$
K_M [16]	$5.39\times10^{-4}\exp(8487/T)\ \ (m^3/kmol)$
K_W [16]	$8.47\times10^{-2}\exp(5070/T)\ (m^3/kmol)$
K [18]	$\exp(-1.7+\frac{3220}{T})$

Mathematical modeling for the fixed bed reactor is based on the following assumptions: (1) The reactor is operated at steady state conditions; (2) Plug flow is taken into account and the gas phase is assumed to behave ideally; (3) Adiabatic condition is employed and heat transfer is ignored; (4) The pressure in the reactor is constant. (5) Concentration and temperature changes are considered only in longitudinal direction.

The mass and energy balance equations are arranged according to diffusion, convection and reaction mechanisms in the reactor:

$$\frac{d^2C_k}{dx^2} - \frac{U}{D_{a,k}}\frac{dC_k}{dx} - \frac{\rho_B v \eta(C_M,T)}{D_{a,k}}(-r) = 0 \quad (3)$$

$$\frac{d^2T}{dx^2} - \frac{U\rho C_p}{K_a}\frac{dT}{dx} - \frac{\rho_B \Delta H \eta(C_M,T)}{K_a}(-r) = 0 \quad (4)$$

Eq. (3) should be written for Methanol and DME and index *k* refers to the components. Eqs. (2), (3) and (4) can be changed to a dimensionless form as follows:

$$\frac{d^2\bar{C}_k}{d\bar{x}^2} - Pe_k\frac{d\bar{C}_k}{d\bar{x}} - \Phi_k^2 v_k \eta(C_M,T)(-R) = 0 \quad (5)$$

$$\frac{d^2\bar{T}}{d\bar{x}^2} - Pe_h\frac{d\bar{T}}{d\bar{x}} - \overline{\Delta H}\eta(C_M,T)(-R) = 0 \quad (6)$$

$$-R = \frac{K_M^2 C_o^2\left(\bar{C}_M^2 - \frac{\bar{C}_D\bar{C}_M}{K}\right)}{\left(1+2\sqrt{K_M\bar{C}_M}+K_W\bar{C}_W\right)^4} \quad (7)$$

where $\overline{C} = \frac{C}{C_0}, \overline{T} = \frac{T}{T_0}, \overline{x} = \frac{x}{L}$. The dimensionless parameters in Eqs. (5) and (6) are:

$$Pe_k = \frac{UL}{D_{a,k}} \quad (8)$$

$$Pe_h = \frac{\rho C_p UL}{K_a} \quad (9)$$

$$\Phi_k^2 = \frac{K_s \rho_B L^2}{D_{a,k} C_0} \quad (10)$$

$$\overline{\Delta H} = \frac{K_s \rho_B L^2 \Delta H}{K_a T_0} \quad (11)$$

The water concentration in each segment can be calculated from the total balance.

$$C_w = C_T - (C_M + C_E) \quad (12)$$

The appearance of the effectiveness factor in Eqs. (5) and (6) is due to the heterogeneity in the reactor and the mass transfer limitation in the catalysts.

We used the results of our previous study to find the effectiveness factor along the reactor [17]. The effectiveness factor was found based on a three dimensional pore network model for the catalyst pellets. In that model pores are places where mass transfer and reaction occurs and nodes are interchange points between the pores. For more details, one can refer to the mentioned study were the effectiveness factor is calculated at different temperatures and methanol concentrations.

Eqs. (5) and (6) are nonlinear equations that can be solved subject to the following boundary conditions:

$$\bar{x} = 0 \qquad \bar{C}_k = \bar{C}_{k,0} \quad (13)$$

$$\bar{x} = 1 \qquad \frac{d\bar{C}_k}{d\bar{x}} = 0 \quad (14)$$

$$\bar{x} = 0 \qquad \bar{T} = \bar{T}_0 \quad (15)$$

$$\bar{x} = 1 \qquad \frac{d\,\bar{T}}{d\bar{x}} = 0 \quad (16)$$

The dispersion coefficient in Eq. (3) should be considered in the porous packed bed. This parameter is a function of Reynolds number and can be calculated as follows [19]:

$$\frac{D_a}{\varepsilon_{bed}} = \frac{D_m}{\tau_{bed}} \qquad \text{Re<1} \quad (17)$$

$$\frac{D_a}{\varepsilon_{bed}} = \frac{D_m}{\tau_{bed}} + 0.5 d_s U \qquad \text{Re>5} \quad (18)$$

The tortuosity in Eqs. (17) and (18) is given by [20]:

$$\tau_{bed} = \frac{1}{\sqrt{\varepsilon_{bed}}} \quad (19)$$

The axial effective thermal conductivity in Eq. (4) is determined by the following equation [21]:

$$\frac{k_a}{k_f} = \frac{k_e^0}{k_f} + 0.5 Re_p Pr \quad (20)$$

where:

$$\frac{k_e^0}{k_f} = \left(\frac{k_p}{k_f}\right)^n \quad (21)$$

where n is:

$$n = 0.28 - 0.757 \log(\varepsilon) - 0.057 \log\left(\frac{k_p}{k_f}\right) \quad (22)$$

The dimensionless parameters in Eq. (20) are:

$$Re_p = \frac{U d_s}{v} \quad (23)$$

$$Pr = \frac{v}{\alpha} \quad (24)$$

The SRK equation of state is used to calculate the compressibility factor [22]. Other parameters used in the simulation are presented in Table. 2.

Table 2: The parameters used in the simulation

Parameter	Value	Parameter	Value
c_p [23]	110 (kJ/kmol K)	k_f	0.1599 (kJ/hr m K)
ΔHr [18]	-23.56 (kJ/mol)	ka [24]	0.42 (kJ/hr m K)
ε_{bed} [16]	0.4	kp [24]	0.972 (kJ/hr m K)
L [16]	0.7 (m)	$\bar{Z}$ [25]	0.99515
d [16]	0.078 (m)	ρ_B [16]	882 (kg_{cat}/m^3)
ρ	0.0825 ($kmol/m^3$)	$D_{a,methanol}$	0.201 (m^2/hr)
d_S [16]	0.003 (m)	$D_{a,DME}$	0.0081 (m^2/hr)

The finite difference method is used to solve Eqs. (5) and (6):

$$[2 - Pe_k \Delta x]\, \bar{C}_{k,i+1} - 4\, \bar{C}_{k,i} + [2 + Pe_k \Delta x]\, \bar{C}_{k,i-1} - 2\Delta x^2 \phi_k^2 v_k \eta(C_M, T)(-R) = 0 \quad (25)$$

$$[2 - Pe_h \Delta x]\, \bar{T}_{i+1} - 4\, \bar{T}_i + [2 + Pe_h \Delta x]\, \bar{T}_{i-1} - 2\Delta x^2 \overline{\Delta H} \eta(C_M, T)(-R) = 0 \quad (26)$$

Where *k* refer to different components (DME and Methanol) and *i* shows the grid number. Δx is the element length in the reactor and here it is considered equal to 0.01 of the reactor length these equation should be written for all the grids. Using the conditions Eqs (13)-(16), the nonlinear set of equations has to be solved in order to calculate the concentration and

temperature distributions in the reactor. A try and error method is used to transform the equations into a linear form. Then the set of linear equations is solved using the LU method. This trial method is repeated until desired precision is obtained.

3. Results and discussion

Fig. 1 shows the methanol concentration versus reactor length. The results are presented for different flow rates and compared to the experimental data. As the flow rate decreases, the residence time will increase and methanol has more time to be in contact with catalysts in the reactor. Therefore, the equilibrium conversion is achieved in a smaller length from the reactor from the inlet.

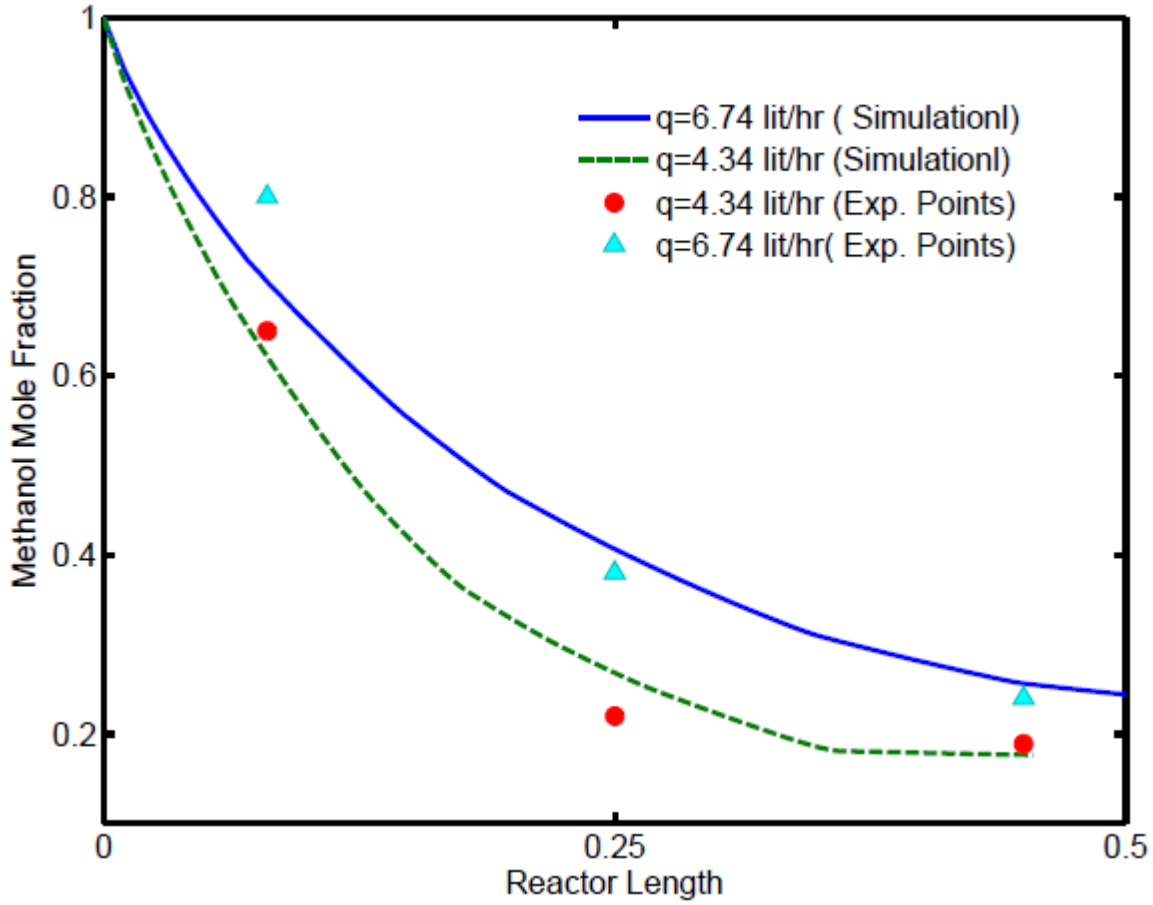

Fig. 1: Methanol mole fraction as a function of reactor length at T_0=551 K

Fig. 2 presents temperature distribution in the reactor at different flow rates at a constant inlet temperature. Increase in flow rate affects the temperature distribution in the reactor and would decrease it along the reactor. In both flow rates equilibrium condition is attained

and the final temperature is the same. However, when the flow rate decreases the final temperature occurs at a distance closer to the reactor inlet.

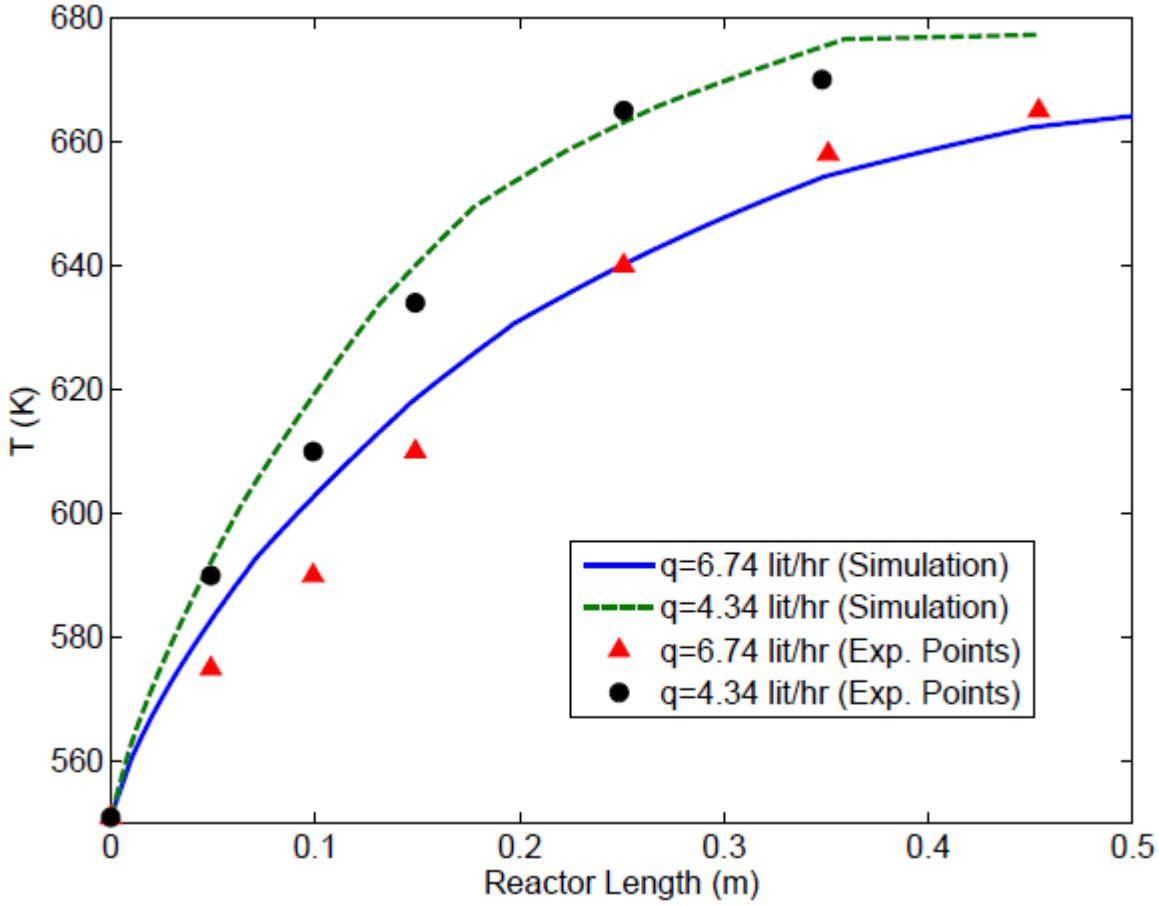

Fig 2: The simulated reactor temperature as a function of reactor length at T_0=551 K

The effect of increase in inlet temperature on methanol concentration distribution in the reactor is demonstrated in Fig. 3 As the inlet temperature increases, the reaction rate would also increase and the equilibrium conversion is attained in a smaller length of the reactor. Therefore, the upper limit of the temperature corresponding to the equilibrium condition is closer to the reactor inlet.

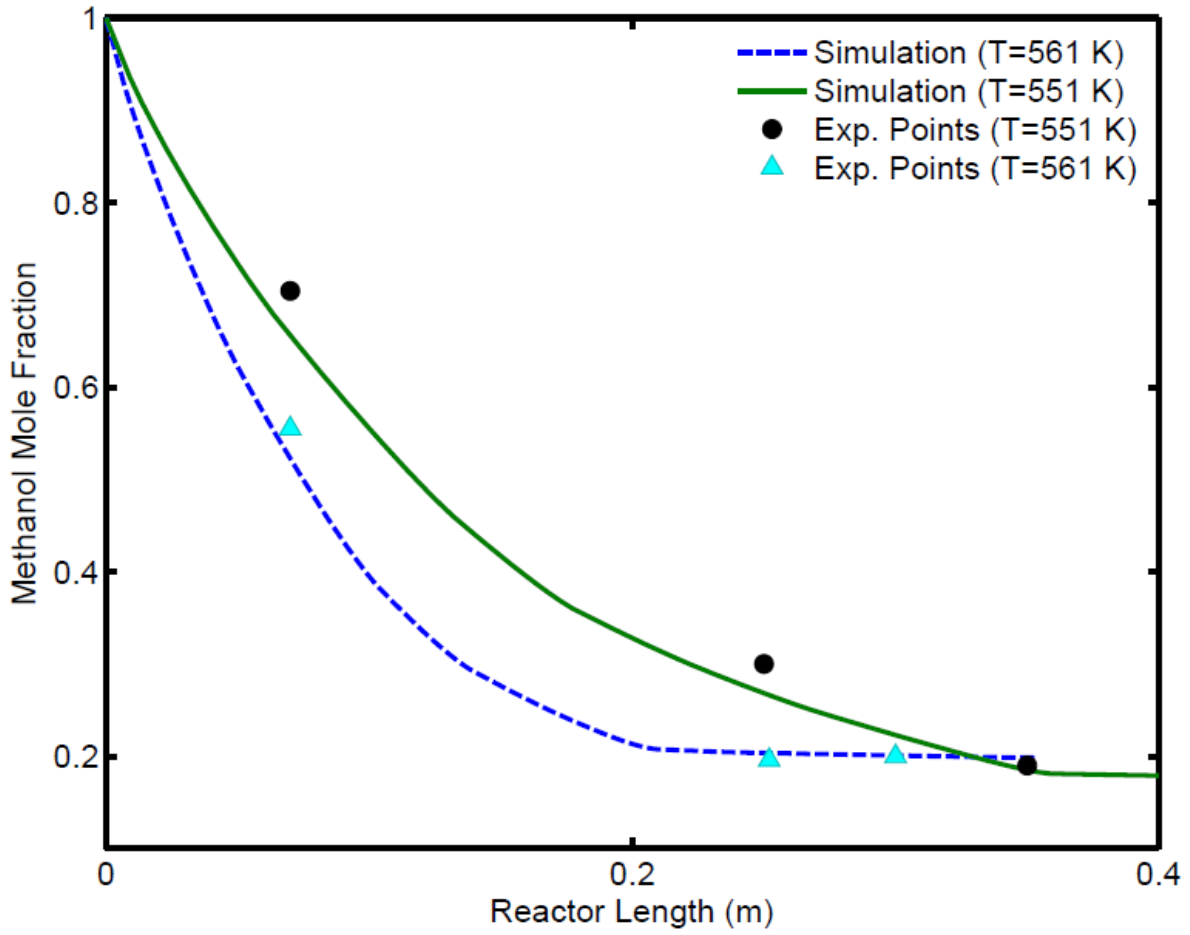

Fig. 3: Methanol mole fraction as a function of reactor length at different inlet temperature

The effect of inlet temperature on temperature distribution in the reactor is also shown in Fig. 4 Higher inlet temperature would increase the reaction rate and therefore the temperature would also be higher along the reactor. The final temperature due to equilibrium condition happens closer to the reactor inlet consequently.

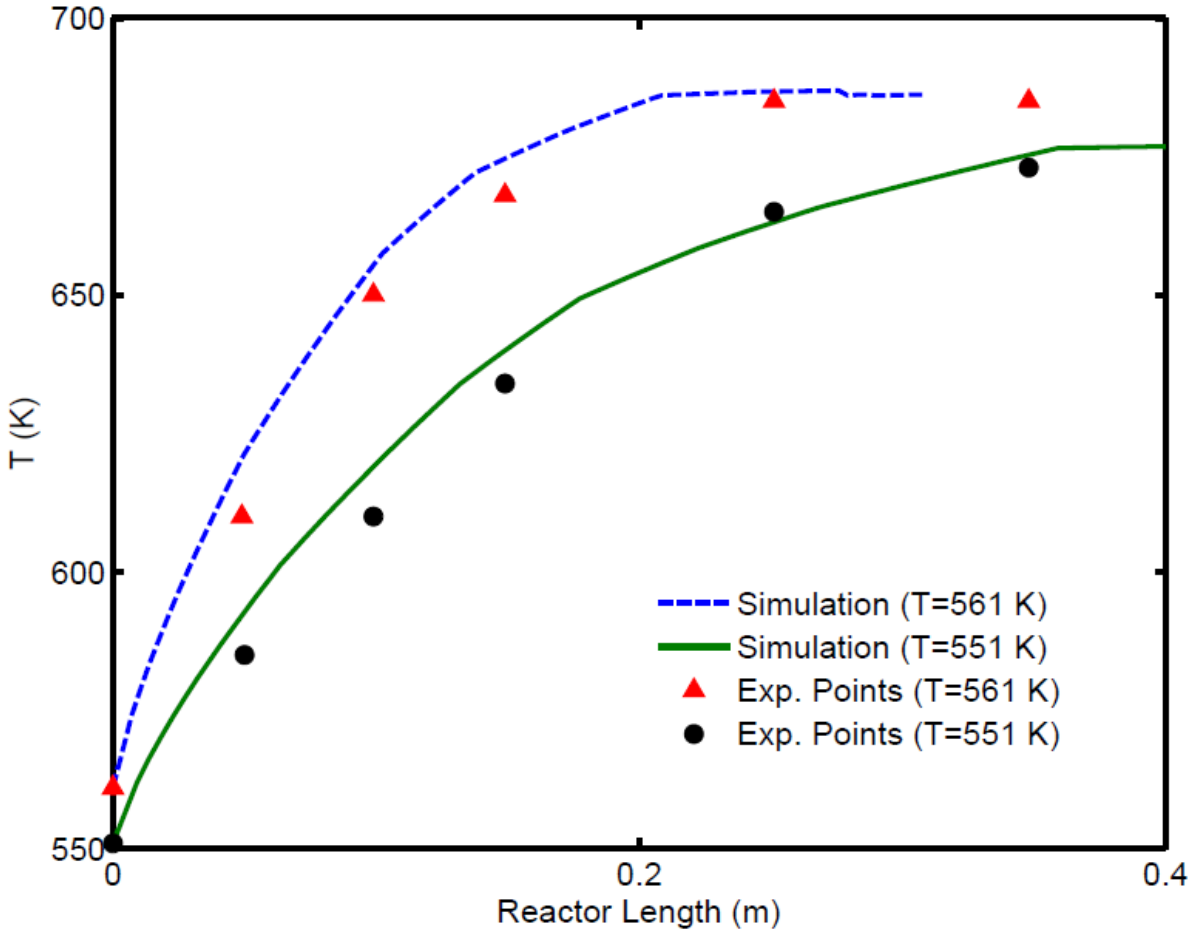

Fig. 4: The simulated reactor temperature as a function of reactor length at different inlet temperature

Fig. 5 presents the concentration distribution of DME, methanol and water along the reactor. As expected DME Concentration increase along the reactor while methanol decrease.

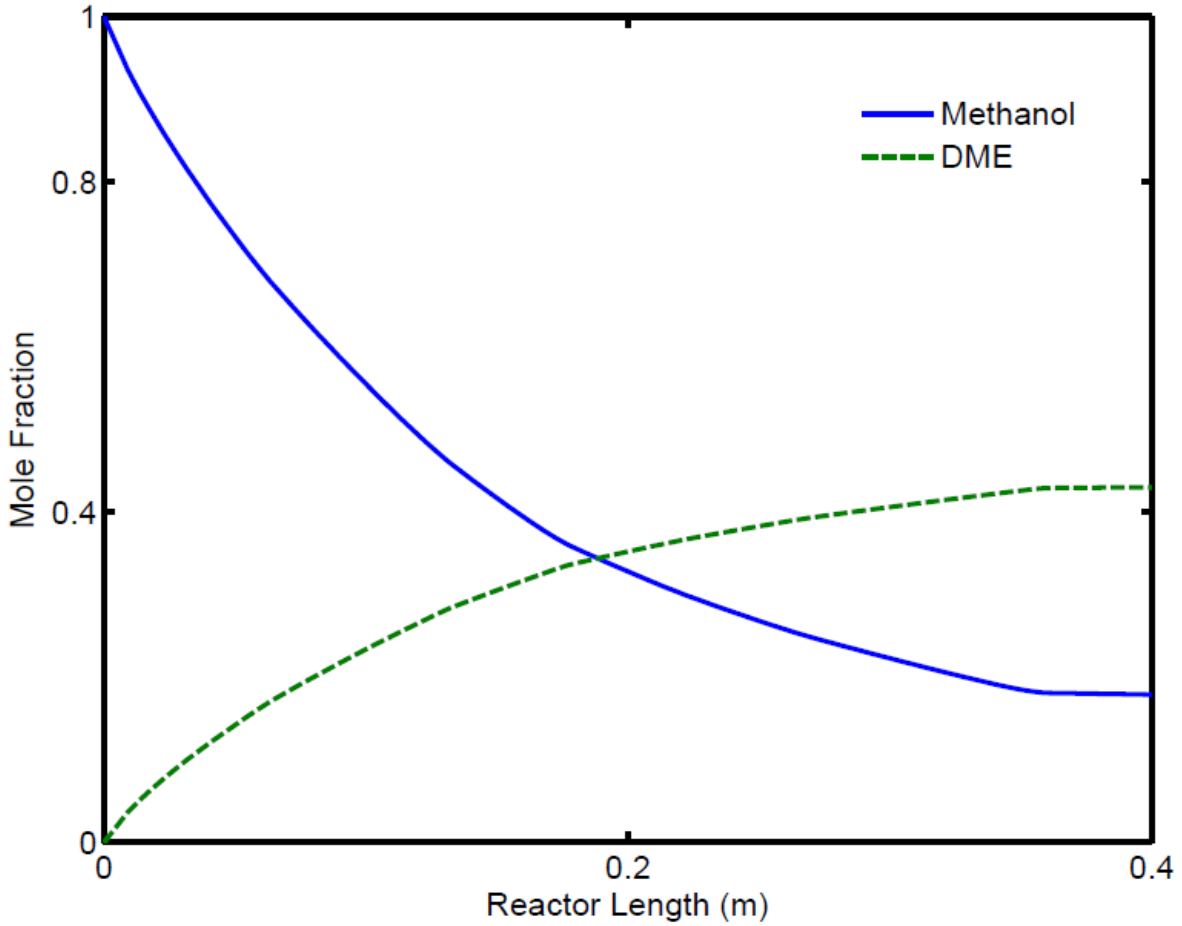

Fig 5: Methanol and DME mole fraction as a function of reactor length at q=4.34 L/hr and at T_0=551 K.

The effect of inlet methanol concentration on concentration distribution in the reactor is studied in Fig. 6 If methanol includes some water at the reactor inlet, DME conversion would strongly reduce. The methanol concentration along the reactor would be higher or in other words the DME concentration would be less as the inlet water. content of methanol increases and the necessary reactor length would increase. Therefore feed water content affects reactor length

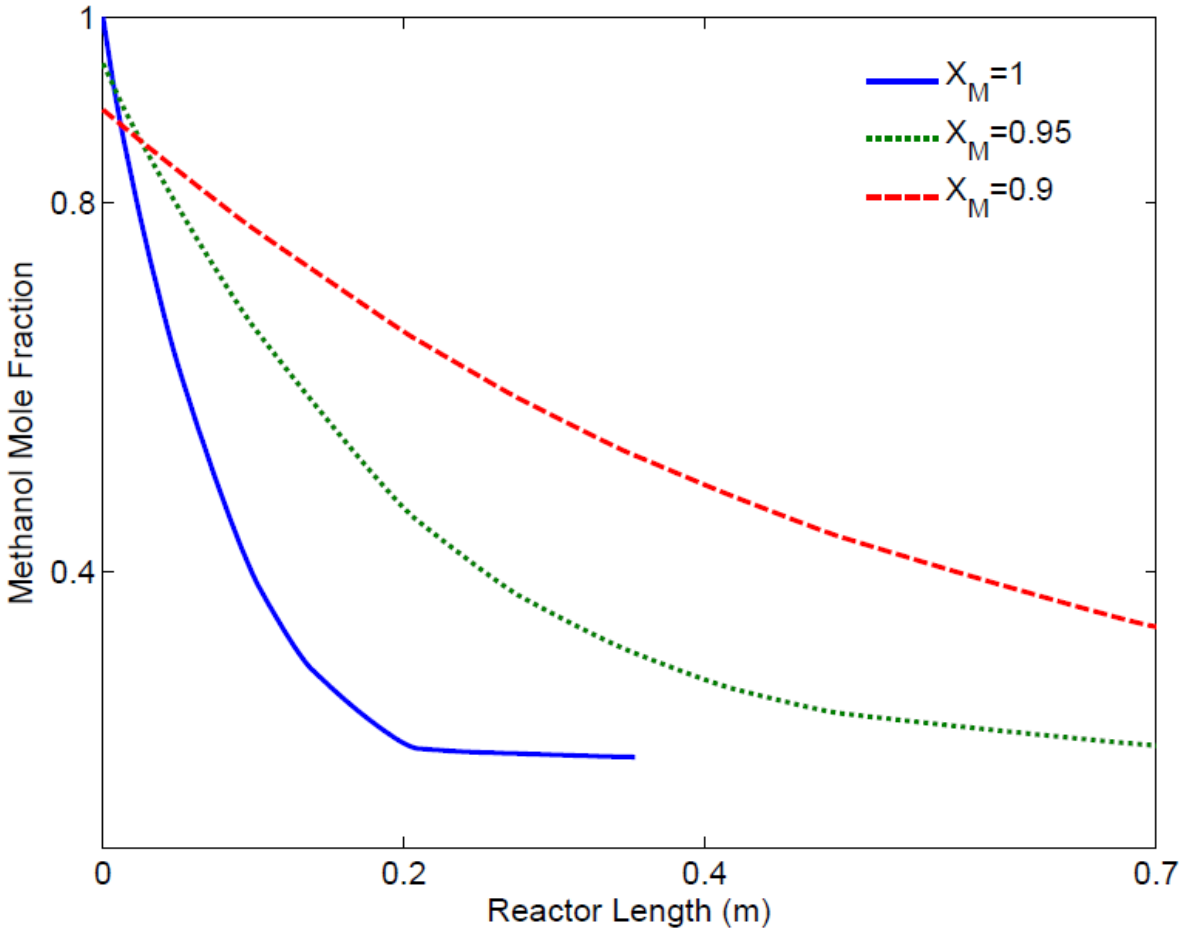

Fig **6**: Methanol mole fraction as a function of reactor length at q=4.34 L/hr and at T_0=561 K for different C_M

4. Conclusion

Modeling and simulation for the methanol dehydration process is studied. The effectiveness factor is considered due to pore network model results for catalyst pellets. The simulations indicate that methanol inlet temperature and its flow rate affect concentration and temperature distribution in the reactor. Increase in inlet temperature and decrease in methanol flow rate causes the equilibrium condition occur in a smaller length from the reactor inlet. The presence of water in the inlet methanol would decrease the reaction rate in the reactor as well.

NOMENCLATURE

C Concentration
C_0 total concentration

c_p	specific heat of fluid
d	reactor diameter
D_a	dispersion coefficient
$D_{a,k}$	dispersion coefficient
D_m	molecular diffusion coefficient
d_s	particle diameter
K	thermodynamic equilibrium constant
K_s	reaction rate constant
K_M	adsorption constant of methanol
K_w	adsorption constant of water
k_a	axial thermal conductivity
k_p	solids thermal conductivity
k_f	fluid thermal conductivity
k_e^0	thermal conductivity of a quiescent bed
L	catalyst bed height
$\mathrm{P}e_k$	Peclet number for k component
$\mathrm{P}e_h$	heat Peclet number
Pr	Prandtle number
T	temperature
T_0	inlet temperature
U	superficial velocity
x	reactor longitudinal coordinate
$\bar{Z}$	
α	thermal diffusivity
ΔH	heat of reaction
$\overline{\Delta H}$	dimensionless heat of reaction
ε_{bed}	bed porosity
$\eta(C_M, T)$	effectiveness factor
ρ	gas phase density
ρ_B	catalyst bed density
τ_{bed}	tortuosity coefficient
υ	kinematic viscosity
Φ_k^2	thiele modulus

Subscripts

d	DME
k	Methanol, DME
M	Methanol
W	water

REFERENCES

1. Arcoumanis, C.; Bae, C.; Crookes, R.; Kinoshita, E., The potential of di-methyl ether (DME) as an alternative fuel for compression-ignition engines: A review. *Fuel* **2008,** *87* (7), 1014-1030.

2. Semelsberger, T. A.; Borup, R. L.; Greene, H. L., Dimethyl ether (DME) as an alternative fuel. *Journal of Power Sources* **2006,** *156* (2), 497-511.

3. Hassanpour, S.; Yaripour, F.; Taghizadeh, M., Performance of modified H-ZSM-5 zeolite for dehydration of methanol to dimethyl ether. *Fuel Processing Technology* **2010,** *91* (10), 1212-1221.

4. Keshavarz, A. R.; Rezaei, M.; Yaripour, F., Nanocrystalline gamma-alumina: A highly active catalyst for dimethyl ether synthesis. *Powder Technology* **2010,** *199* (2), 176-179.

5. Lu, W.-Z.; Teng, L.-H.; Xiao, W.-D., Simulation and experiment study of dimethyl ether synthesis from syngas in a fluidized-bed reactor. *Chemical Engineering Science* **2004,** *59* (22), 5455-5464.

6. Moradi, G. R.; Ahmadpour, J.; Yaripour, F., Intrinsic kinetics study of LPDME process from syngas over bi-functional catalyst. *Chemical Engineering Journal* **2008,** *144* (1), 88-95.

7. Moradi, G. R.; Nazari, M.; Yaripour, F., The interaction effects of dehydration function on catalytic performance and properties of hybrid catalysts upon LPDME process. *Fuel Processing Technology* **2008,** *89* (12), 1287-1296.

8. Yaripour, F.; Baghaei, F.; Schmidt, I.; Perregaard, J., Catalytic dehydration of methanol to dimethyl ether (DME) over solid-acid catalysts. *Catalysis Communications* **2005,** *6* (2), 147-152.

9. Yaripour, F.; Mollavali, M.; Jam, S. M.; Atashi, H., Catalytic Dehydration of Methanol to Dimethyl Ether Catalyzed by Aluminum Phosphate Catalysts. *Energy & Fuels* **2009,** *23* (4), 1896-1900.

10. Hassanpour, S.; Taghizadeh, M.; Yaripour, F., Preparation, Characterization, and Activity Evaluation of H-ZSM-5 Catalysts in Vapor-Phase Methanol Dehydration to Dimethyl Ether. *Industrial & Engineering Chemistry Research* **2010,** *49* (9), 4063-4069.

11. Bandiera, J.; Naccache, C., Kinetics of methanol dehydration on dealuminated H-mordenite: Model with acid and basic active centres. *Applied Catalysis* **1991,** *69* (1), 139-148.

12. Bercic, G.; Levec, J., Intrinsic and global reaction rate of methanol dehydration over .gamma.-alumina pellets. *Industrial & Engineering Chemistry Research* **1992,** *31* (4),

1035-1040.

13. Figueras, F.; Nohl, A.; de Mourgues, L.; Trambouze, Y., Dehydration of methanol and tert-butyl alcohol on silica-alumina. *Transactions of the Faraday Society* **1971,** *67* (0), 1155-1163.

14. Gates, B. C.; Johanson, L. N., The dehydration of methanol and ethanol catalyzed by polystyrene sulfonate resins. *Journal of Catalysis* **1969,** *14* (1), 69-76.

15. Klusáček, K.; Schneider, P., Stationary catalytic kinetics via surface concentrations from transient data: Methanol dehydration. *Chemical Engineering Science* **1982,** *37* (10), 1523-1528.

16. Bercic, G.; Levec, J., Catalytic dehydration of methanol to dimethyl ether. Kinetic investigation and reactor simulation. *Industrial & Engineering Chemistry Research* **1993,** *32* (11), 2478-2484.

17. Beigi, H.; Dadvar, M.; Halladj, R., Pore network model for catalytic dehydration of methanol at particle level. *AIChE Journal* **2009,** *55* (2), 442-449.

18. Schiffino, R. S.; Merrill, R. P., A mechanistic study of the methanol dehydration reaction on .gamma.-alumina catalyst. *The Journal of Physical Chemistry* **1993,** *97* (24), 6425-6435.

19. Berger, R. J.; Pérez-Ramírez, J.; Kapteijn, F.; Moulijn, J. A., Catalyst performance testing: Radial and axial dispersion related to dilution in fixed-bed laboratory reactors. *Applied Catalysis A: General* **2002,** *227* (1), 321-333.

20. Epstein, N., On tortuosity and the tortuosity factor in flow and diffusion through porous media. *Chemical Engineering Science* **1989,** *44* (3), 777-779.

21. Wen, D.; Ding, Y., Heat transfer of gas flow through a packed bed. *Chemical Engineering Science* **2006,** *61* (11), 3532-3542.

22. Prausnitz, J. M.; Thaler, R. L.; Azeredo, E. G., *Molecular Thermodynamics of fluid phase Equilibria*. Second ed.; Prentic Hall: 1988.

23. Diep, B. T.; Wainwright, M. S., Thermodynamic equilibrium constants for the methanol-dimethyl ether-water system. *Journal of Chemical & Engineering Data* **1987,** *32* (3), 330-333.

24. Bercic, G. Dehydration of methanol over gamma alumina kinetics of reaction and mathematical model of an industrial reactor. University of Ljubljana, 1990.

25. Walas, S. M., *Phase Equilibria in Chemical Engineering*. Butterworth-Heinemann:

1985.

Figures

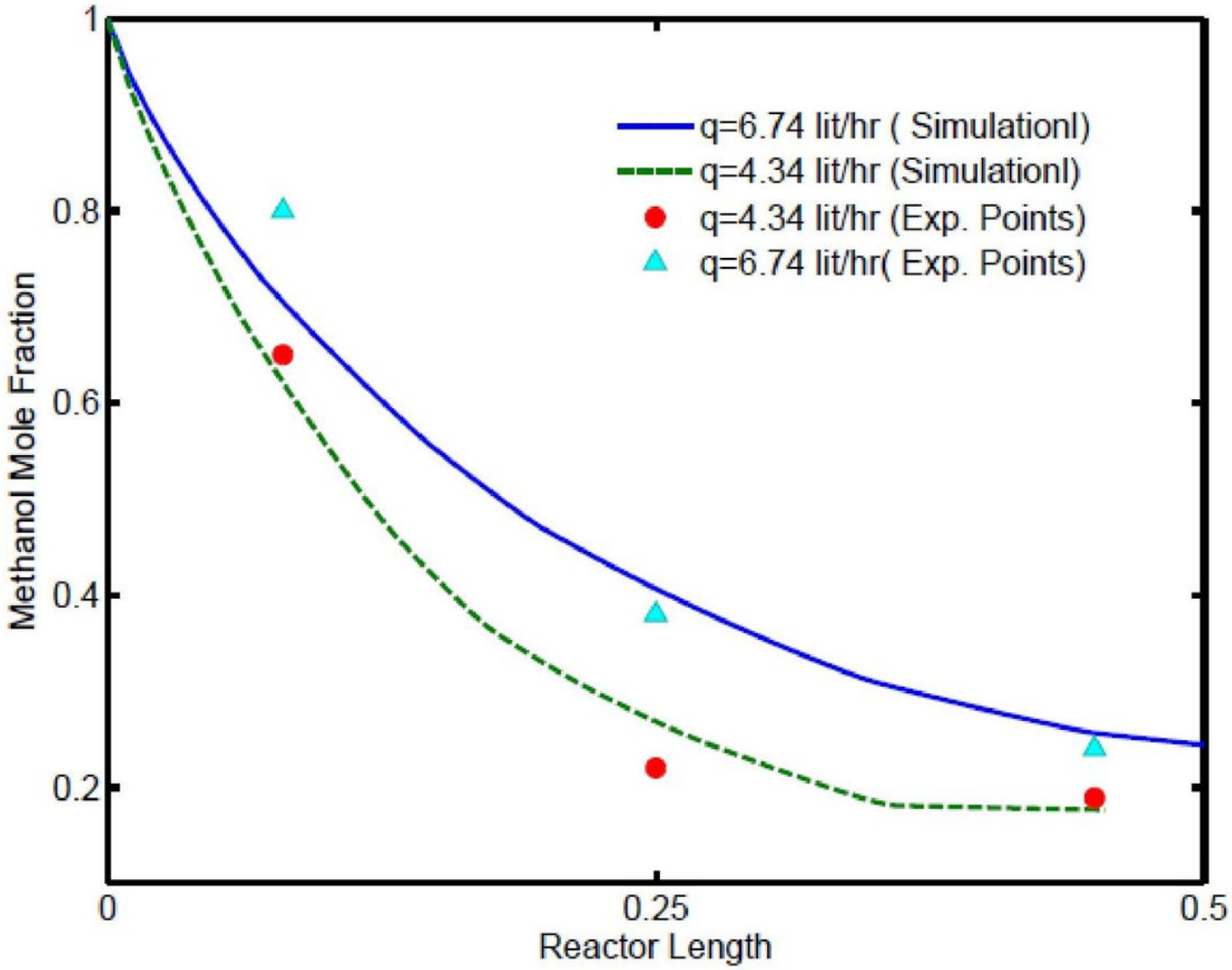

Figure 1

Methanol mole fraction as a function of reactor length at T0=551 K

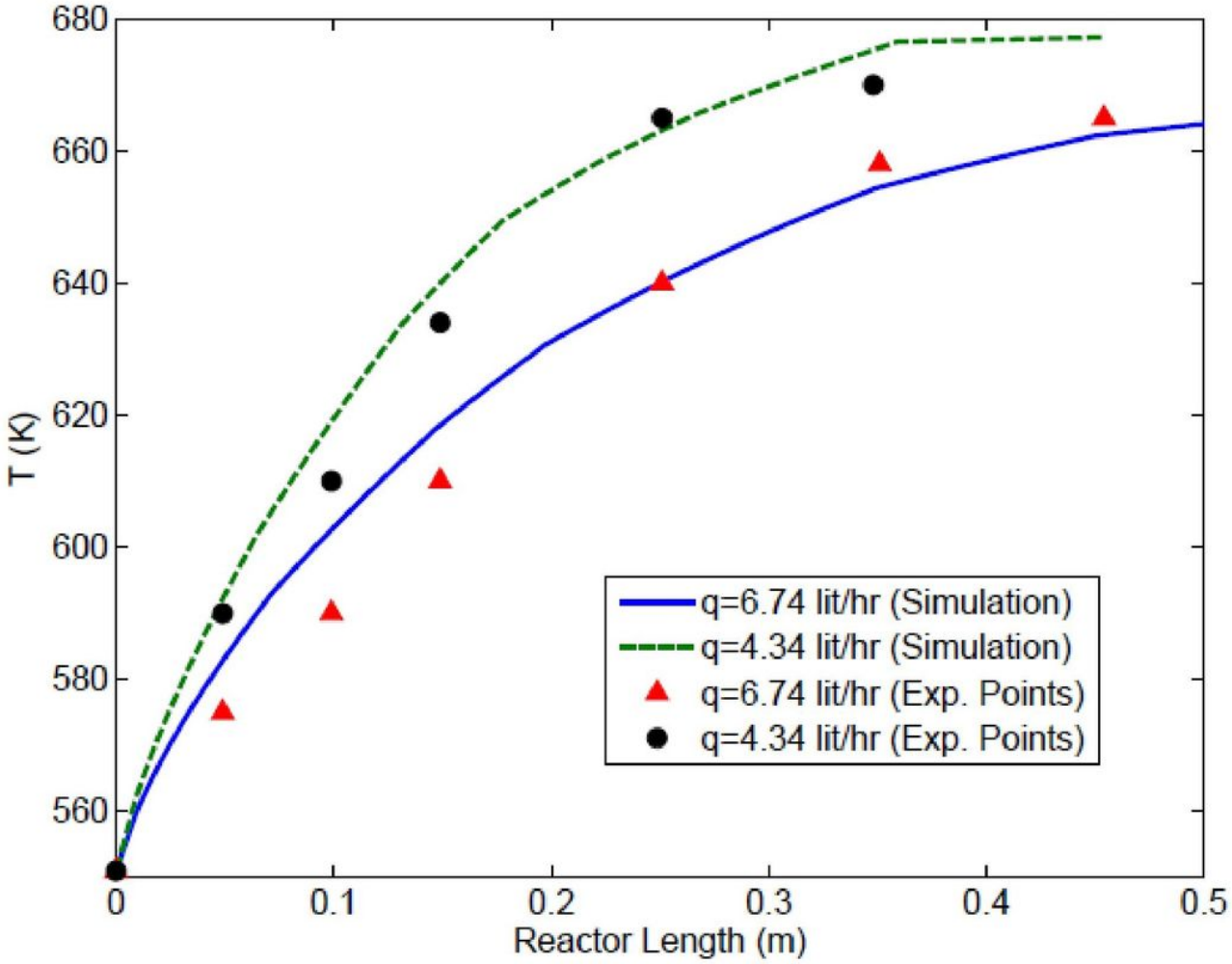

Figure 2

The simulated reactor temperature as a function of reactor length at T0=551 K

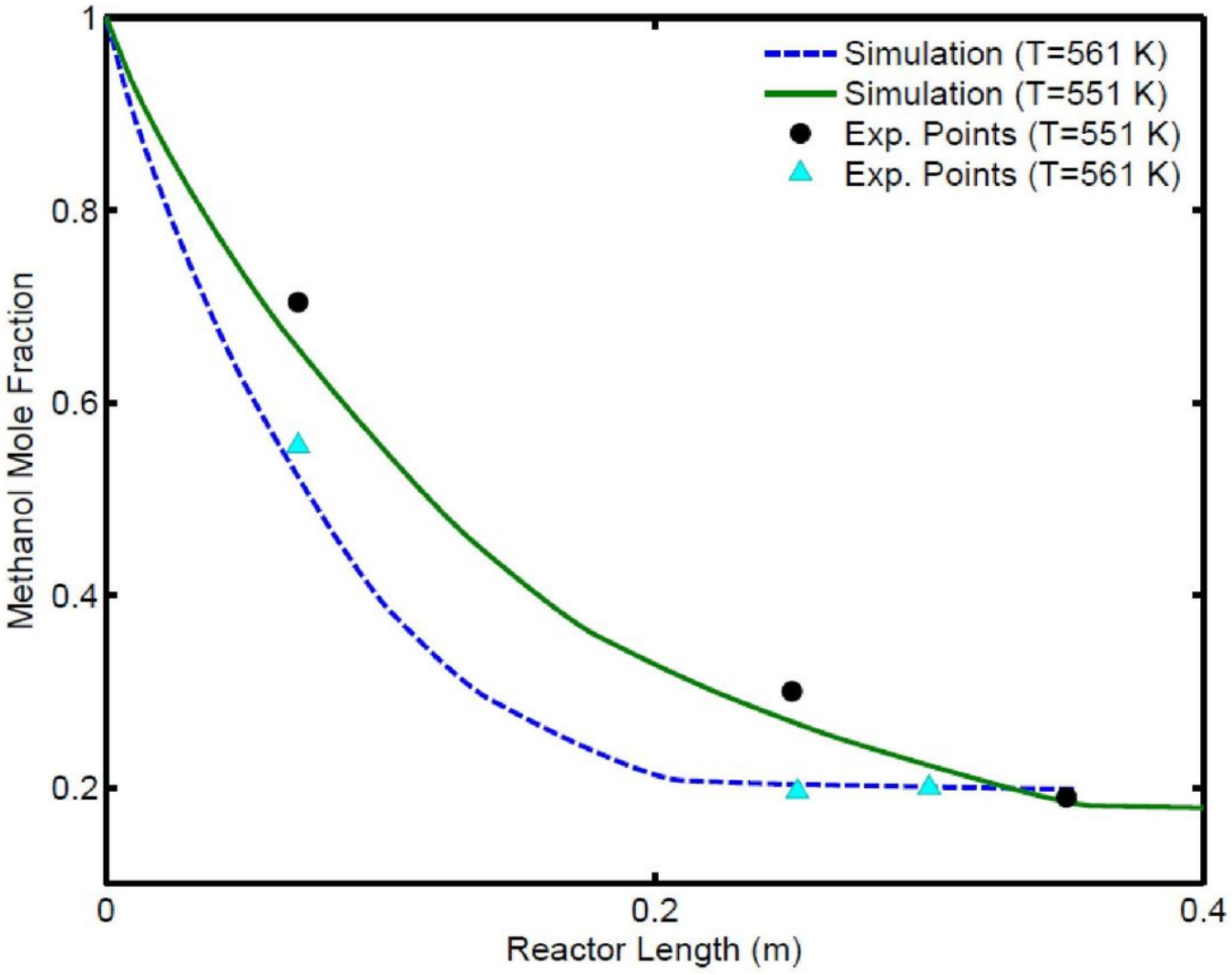

Figure 3

Methanol mole fraction as a function of reactor length at different inlet temperature

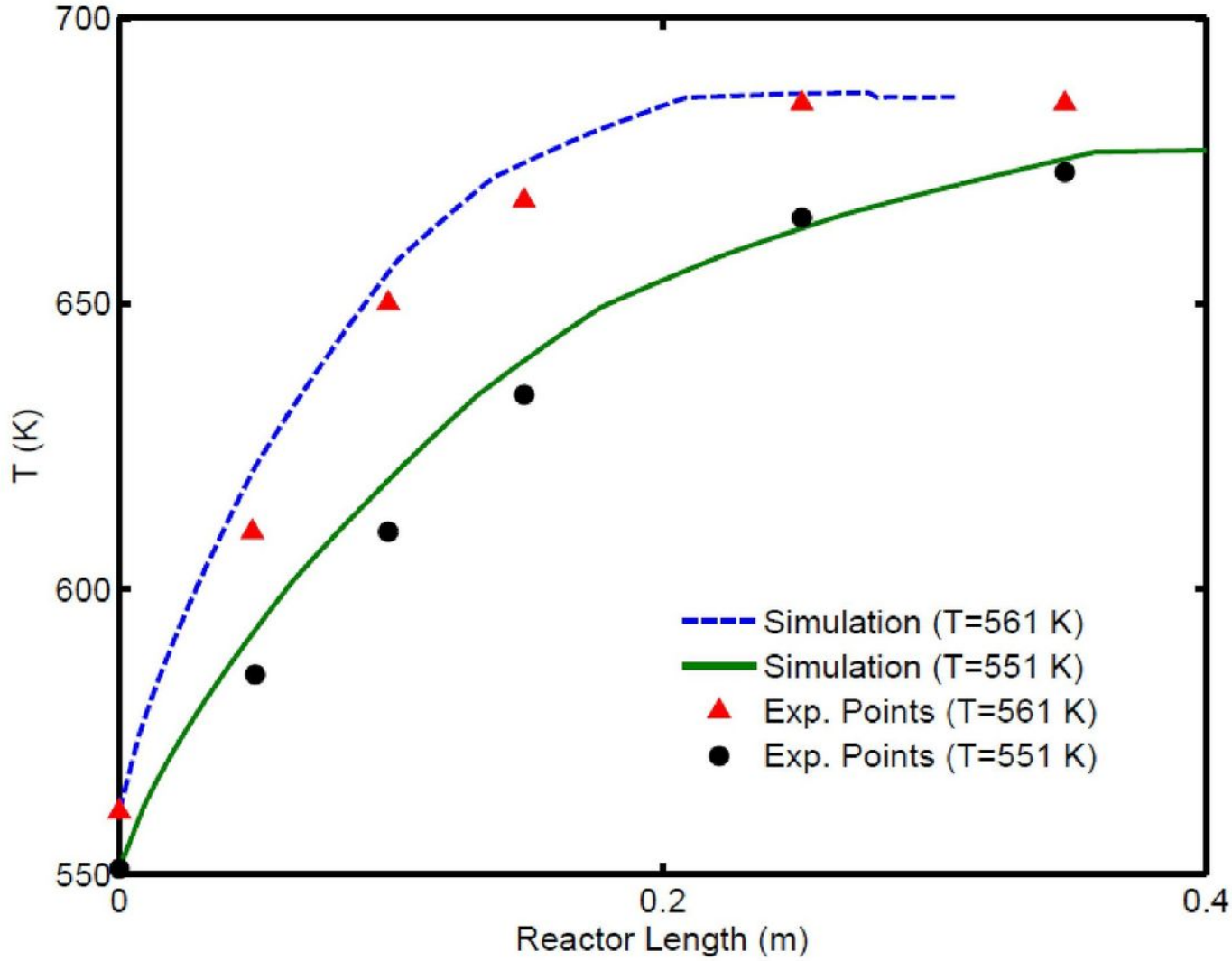

Figure 4

The simulated reactor temperature as a function of reactor length at different inlet temperature

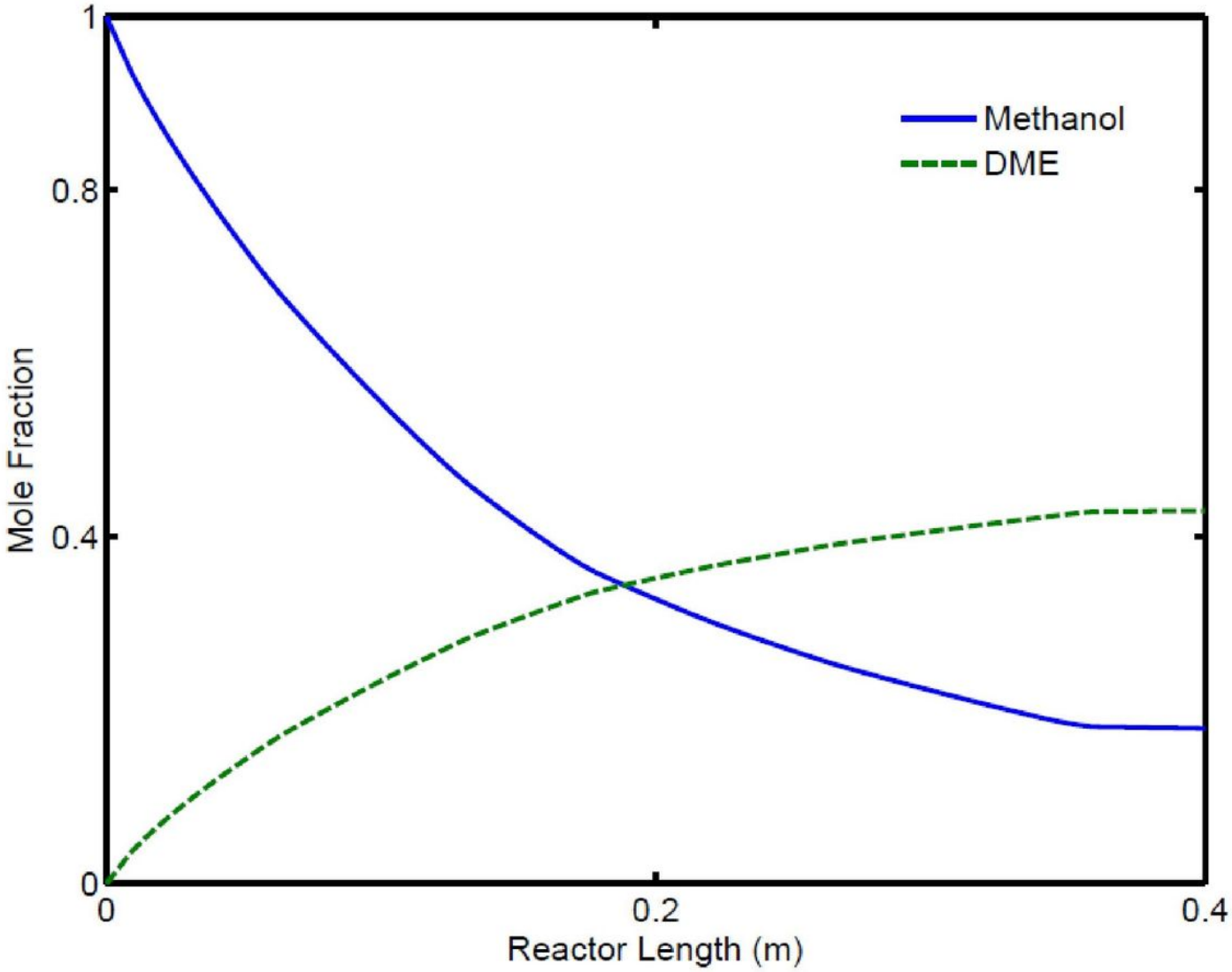

Figure 5

Methanol and DME mole fraction as a function of reactor length at q=4.34 L/hr and at T0=551 K.

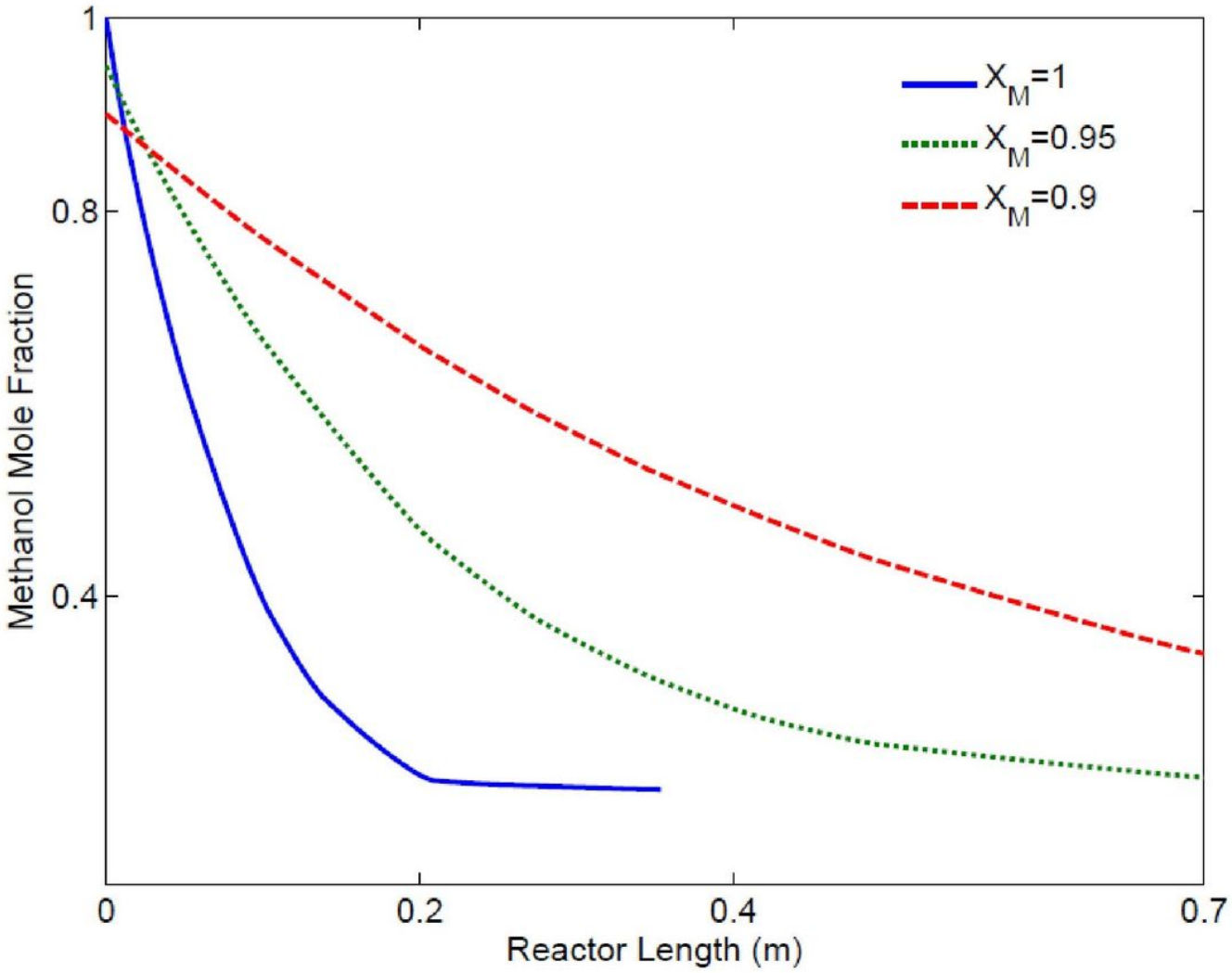

Figure 6

Methanol mole fraction as a function of reactor length at q=4.34 L/hr and at T0=561 K for different CM